Article

Synthesis of a Poly(3-dodecylthiophene) Bearing Aniline Groups for the Covalent Functionalization of Carbon Nanotubes

Felipe Wasem Klein [1,2], Jean-Philippe Lamps [1], Matthieu Paillet [2] , Pierre Petit [1,*] and Philippe J. Mésini [1,*]

[1] Université de Strasbourg, CNRS, Institut Charles Sadron, 23 rue du Loess, F67000 Strasbourg, France; felipe.wasem-klein@ics-cnrs.unistra.fr (F.W.K.); jean-philippe.lamps@ics-cnrs.unistra.fr (J.-P.L.)

[2] Laboratoire Charles Coulomb (L2C), Université de Montpellier, CNRS, F34095 Montpellier, France; matthieu.paillet@umontpellier.fr

* Correspondence: petit@ics-cnrs.unistra.fr (P.P.); mesini@ics-cnrs.unistra.fr (P.J.M.)

Abstract: The functionalization of carbon nanotubes by polymers necessitates two steps, first their modification by oxidizing them or by covalently attaching small compounds to them, then the growth of the polymer chains from these anchors or their grafting onto them. In order to better control the process and the rate of functionalization, we develop polymers able to covalently react with the carbon nanotubes by their side chains in one step. We describe the synthesis of a copolymer of dodecylthiophene and its analogue bearing an aniline group at the end of the dodecyl side chain. This copolymer can functionalize single-walled carbon nanotubes (SWNTs) non-covalently and disperse more SWNTs than its hexyl analogues. UV-Vis and fluorescence spectroscopies show that in these non-covalent hybrids, the polymer forms p-stacked aggregates on the SWNTs. The non-covalent hybrids can be transformed into covalent ones by diazonium coupling. In these covalent hybrids the polymer is no longer p-stacked. According to Raman spectroscopy, the conformation of the poly(3-hexylthiophene) backbone is more ordered in the non-covalent hybrids than in the covalent ones.

Keywords: carbon nanotubes; alkylation; diazonium; polythiophene; photoluminescence; Raman spectroscopy

1. Introduction

Covalent functionalization of carbon nanotubes has proved to be efficient to endow them with new properties, such as enhanced solubility [1,2], compatibilization in polymer matrices [3–5], and photoluminescence [6,7]. One of the main procedures for covalent functionalization is the diazonium coupling reaction, which presents a high efficiency [8], a good control [7,9], and can be adapted to different environments [10]. Most notably, this reaction is capable of attaching aryl groups even to polymer-wrapped carbon nanotubes [11], overcoming the steric hindrance of the dispersing agent. In most functionalization methods, the nanotubes are first functionalized by oxidation or by reaction with small compounds such as aniline derivatives [12–14]. Then polymers are grown from those reactive anchors or grafted onto them. However, this synthetic scheme comprises two steps, which limits the control of the functionalization rate.

In order to overtake this problem, we propose a functionalization in one-step by attaching the functional group directly to the polymer chain. In our previous work, [15] we have synthesized PHT*co*AHT, a statistical copolymer based on poly(3-hexylthiophene) and bearing aniline side groups. This copolymer forms non-covalent hybrids with single-walled carbon nanotubes (SWNTs) and can also react with the SWNTs in one step to form covalent hybrids. The synthesis had been designed to yield the polymer with high regioregularity, notably with no detectable head-to-head arrays. This regioregularity favors

planar conformation and has enabled us to study the conformation of main chains in both types of hybrids. These have very different structures: in the non-covalent hybrids the polymer forms aggregates of few extended planar chains interacting through π-π interactions with SWNTs; in the covalent ones the polymer does not π-stack on the SWNTs and does not form aggregates on their walls, and as shown by Raman spectroscopy, the main chain is disordered like in regiorandom P3HT. These differences between both hybrids are attributed to the aniline appended chains which, in the covalently grafted ones, act as a spacer between the SWNTs and the PHT*co*AHT backbone.

Moreover, with these functionalized polymers we have observed only a very low amount of functionalized SWNTs in the final suspensions. A possible reason for this limited yield is the relatively low capacity of P3HT to exfoliate SWNTs in THF. The length of the side chains may influence the formation and the structure of the hybrids. Indeed, it has been observed with other conjugated copolymers [16–18], that longer side-chains can disperse larger amounts of nanotubes. In this context, we describe the synthesis of a new polymer bearing aniline side groups, but with longer side chains: a copolymer of 3-dodecylthiophene and its aniline appended derivative. SWNTs were functionalized covalently and non-covalently with this copolymer. The resulting hybrids were studied by UV-Vis-NIR, fluorescence and Raman spectroscopies.

2. Materials and Methods

2.1. General Methods

NMR spectra were recorded on a WH-400 MHz spectrometer from Bruker (Wissembourg, France) and were reported in δ ppm relative to Me$_4$Si. The FTIR spectra were recorded on a Vertex 70 spectrometer (Bruker Optics, Karlsruhe, Germany) equipped with an ATR diamond reflection unit.

Size exclusion chromatography: analytical and preparative SEC were carried out according the previously described procedure [15].

UV–Vis–NIR spectra were recorded with a Cary 5000 (Varian, Palo Alto, CA, USA) or a Lambda 25 spectrometer (Perkin-Elmer, Villebon, France).

Fluorescence spectra were measured with a E348 fluorimeter from HORIBA-Jobin-Yvon (Palaiseau, France). The suspensions characterized by UV-Vis (with rather high absorbance) have been analyzed with a triangular cell to avoid internal filter effects.

Raman spectra were recorded using an Acton SP2500 spectrometer fitted with a PyLoN CCD detector and a 1800 grooves per mm grating (Teledyne Princeton Instrument, Trenton, NJ, USA). The samples were excited at 633 nm (1.96 eV) using a He-Ne laser through a 50 × objective (Numerical Aperture 0.5) and 0.1 mW impinging on the sample.

2.2. Synthesis of the Monomers

2-(12-bromododecyl)oxy)tetrahydro-2*H*-pyran (3): Amberlyst 15® resin (3 g) was suspended in a solution of 12-bromododecanol (5 g, 18.9 mmol) in CH$_2$Cl$_2$ (50 mL) under Ar. 3,4-dihydro-2*H*-pyran (1.74 g, 20.7 mmol) was added and the suspension was stirred 90 min at 20 °C. The resin was filtered and the medium evaporated under vacuum. The raw product was purified by chromatography (SiO$_2$, cyclohexane/AcOEt 96/4 *v/v*) to yield pure **3** as a colorless oil (4.91 g, 74% yield). ^{1}H NMR (400 MHz, CDCl$_3$) d (ppm): 4.58 (dd, *J* = 4.6, 2.7 Hz, 1H, OCHO), 3.88 (1 H, pyran C**H**HO), 3.74 (dt, *J* = 9.6, 6.8 Hz, 1H, CH**H**-OTHP), 3.47 (m, 1H, pyran CH**H**O), 3.40–3.34 (m, 3H, C**H**H-OTHP + CH$_2$Br), 1.89–1.33 (m, 24H, CH$_2$). ^{13}C NMR (100 MHz, CDCl$_3$) d (ppm): 98.9 (OCHO), 67.8 (dodec. CH$_2$O), 62.3 (pyran CH$_2$O), 34.1 (CH$_2$-Br), 32.9 (**C**H$_2$CH$_2$Br), 30.9 (pyran C3), 29.8,29.63, 29.61, 29.58, 29.55, 29.50, 28.8 (dodec.C9), 28.3 (dodec. C10), 26.3 (dodecyl C3), 25.7 (pyranC4), 19.8 (pyran C5). FTIR (solid, ATR diamond) ν (cm^{-1}): 2923 (ν$_{as}$CH$_2$), 2853 (ν$_s$CH$_2$), 1465, 1453, 1440, 1352, 1260, 1200, 1162, 1134, 1120, 1077, 1032, 1021. HRMS (ESI Na$^+$): *m/z*: 371.1576 (MNa$^+$), calcd for C$_{17}$H$_{33}$BrO$_2$: 371.1556. Elem. Anal. C 58.40, H 9.58; calcd for C$_{17}$H$_{33}$BrO$_2$: C 58.45, H 9.52.

3-(12-(tetrahydro-2*H*-pyran-2-oxy)dodecyl)thiophene (4): A suspension of magnesium turnings (0.38 g, 15.7 mmol, 1.1 eq.) in anhydrous THF (25 mL) was heated at 50 °C and a chip of iodine was added. Ten percent of the total amount of **3** (5 g, 14.3 mmol) was introduced and heated 2 h 30. When Mg started to react, the rest of **3** was added dropwise and the mixture heated until most of the Mg has been consumed. The organomagnesium solution was cooled at 20 °C and kept under Ar. In a separate flask, a solution of 3-bromothiophene (2.8 g, 17.2 mmol, 1.1 equiv.) and Ni(dppp)Cl2 (0.39 g, 715 µmol, 0.05 equiv.) in anhydrous THF (25 mL) were stirred at 25 °C under Ar. The organomagnesium solution was added dropwise and the resulting mixture heated at reflux for 30 h. The reaction was quenched with water and extracted with cyclohecxane/EtOAc (1/1 *v/v*, 3 × 5 mL). The combined organic layers were dried (MgSO4) and concentrated under vacuum. The crude was purified by chromatography (SiO2, cyclohexane/EtOAc 96/4 *v/v*) to afford an oil containing 85% of the desired compound **4**, 7% of $C_{12}H_{25}OTHP$ and 8% of $BrC_{12}H_{24}OTHP$, that was used as is in next step (3.93 g, 69% yield, taking into account impurities). ^{1}H NMR (400 MHz, CDCl3): d (ppm): 7.26 (dd, *J* = 4.9, 3.0 Hz, 1H, thiophene H5), 6.95–6.91 (m, 2H, thiophene H2 and H4), 4.58 (dd, *J* = 4.4, 2.7 Hz, 1H, OCHO), 3.85 (m, 1H, pyran C**H**HO), 3.72 (dt, *J* = 9.6, 6.8 Hz, 1H, C**H**H-OTHP), 3.48 (m, 1H, pyran CH**H**O), 3.37 (dt, *J* = 9.6, 6.6 Hz, 1H, CH**H**-OTHP), 2.65 (t, *J* = 7.3 Hz, 2H, thiophene-CH2), 1.89–1.79 (m, 1H, THP C3-**H**H), 1.78–1.48 (m, 18H, CH2), 1.45–1.30 (m, 8H, CH2).

3-(12-bromododecyl)thiophene (5): A solution of unpurified **4** (100 mg, 284 µmol) and CBr4 (132 mg, 397 µmol, 1.4 equiv.) in anhydrous CH2Cl2 (5–10 mL) is stirred at 0 °C under Ar. PPh3 (208 mg, 793 µmol, 2.8 equiv.) was added, the mixture warmed to 25 °C and stirred for 12 h. The mixture was filtered on Celite®, poured in Et2O, filtered again, and evaporated under vacuum. The crude was purified by chromatography (SiO2, EtOAc/cyclohexane 2/98 *v/v*) to afford pure **5** as an oil (69 mg, 73% yield). ^{1}H NMR (400 MHz, CDCl3) d (ppm): 7.24 (dd, *J* = 4.9, 3.0 Hz, 1H, thiophene H5), 6.94 (m, 2H, thiophene H2 and H4), 3.14 (t, *J* = 6.9 Hz, 2H, CH2Br), 2.64 (t, *J* = 7.8 Hz, 2H, thiophene-CH2), 1.86 (m, 2H, dodecyl C**H2**CH2Br), 1.63 (m, 2H, dodecyl C2-H2), 1.24 (C10-H2), 1.19–1.38 (m, 14H, dodecyl C3-C9-H2). ^{13}C NMR (100 MHz, CDCl3) d (ppm): 143.0 (thiophene C3), 128.3 (thiophene C4), 125.3 (thiophene C5), 120.0 (thiophene C2), 34.2 (CH2Br), 33.0 (**CH2**CH2Br), 30.7 (dodecyl C3), 30.4 (dodecyl C2), 29.9 (dodecyl C9), 29.73, 29.71, 29.67, 29.61, 29.59, 29.5 (dodecyl C7) 28.9 (dodecyl C9), 28.3 (dodecyl C10). HRMS (ESI+): *m/z*: 331.1083 (MH+); calcd for $C_{16}H_{27}BrS$ 331.1090. Elem. anal. C 58.05, H 8.28; calcd for $C_{16}H_{27}BrS$: C 58.00; H 8.21.

2-Bromo-3-(12-bromododecyl)thiophene (6): A solution of **5** (174 mg, 513 µmol, 1 equiv.) and AcOH (1.5 mL) in CHCl3 (5 mL) was stirred at 0 °C under Ar. A solution of *N*-bromosuccinimide (91.3 mg, 0.103 mmol, 1 equiv.) in CHCl3 (1.8 mL) was added in fractions of 5 mL spaced by 15 min. After disappearance of **5** (followed by TLC), the solution was neutralized with a 2 M NaOH solution, mixed with water (10 mL) and extracted with EtOAc (3 × 40 mL). The organic phases were dried (MgSO4) and concentrated under vacuum. The crude was purified by flash chromatography (SiO2, cyclohexane) to afford pure **7** as a yellow oil (90 mg, 43% yield). ^{1}H NMR (400 MHz, CDCl3) d (ppm): 7.20 (d, *J* = 5.6 Hz, 1H, thiophene H5), 6.80 (d, *J* = 5.6 Hz, 1H, thiophene H4), 3.42 (t, *J* = 6.9 Hz, 2H, CH2Br), 2.57 (t, *J* = 7.6 Hz, 2H, thiophene -CH2), 1.87 (p, 2H, *J* = 7.0 Hz, dodecyl C11-H2), 1.52–1.64 (m, 2H, hexyl C2-H2), 1.38–1.50 (m, 2H, dodecyl C10-H2), 1.23–1.38 (m, 14H, dodecyl C3-C9-H2). ^{13}C NMR (100 MHz, CDCl3) δ (ppm): 142.1 (thiophene C3), 128.4 (thiophene C4), 125.3 (thiophene C2), 108.9 (thiophene C5), 34.2 (CH2Br), 33.0 (dodecyl C11), 29.9 (dodecyl C1), 29.72, 29.67, 29.57, 29.54, 29.4 (dodecyl C7), 28.9 (dodecyl C9), 28.3 (dodecyl C10). HRMS (ESI+): *m/z*: 455.9973 (MH+); calcd for $C_{16}H_{26}Br_2S$ 455.9978. Elem. anal. C 46.61, H 6.53; calc. for $C_{16}H_{26}Br_2S$: C 46.84, H 6.39.

2-Bromo-3-(12-bromododecyl)-5-iodothiophene (2): A solution of **6** (200 mg, 483 µmol) and acetic acid (1.5 mL) in CHCl3 (5 mL) was stirred at 0 °C under Ar. *N*-Iodosuccinimide (108 mg, 483 µmol, 1 equiv.) was added. When **7** was no longer detected by TLC, the mixture was mixed with aq. NaOH (3 M, 25 mL) and extracted with CHCl3 (2 × 10 mL). The

organic phase was washed with aq. $Na_2S_2O_3$, dried ($MgSO_4$) and evaporated. The crude was chromatographed (SiO_2, cyclohexane) to yield pure **2** as a solid (210 mg, 81% yield). ^{1}H NMR (CDCl$_3$, 400 MHz) δ (ppm): 6.97 (s, 1H, thiophene H4), 3.41 (t, 2H, *J* = 6.9 Hz, CH$_2$Br), 2.53 (p, *J* = 7.5, 15.0 Hz, 2H, thiophene-CH$_2$), 1.86 (m, 2H, dodecyl C11-H$_2$), 1.53 (p, *J* = 7.6 Hz, 2H, dodecyl C2-H$_2$), 1.50–1.40 (m, 2H, dodecyl C3-H$_2$), 1.12–1.34 (m, 14H, dodecyl C4-C10-H$_2$). ^{13}C NMR (CDCl$_3$, 100 MHz) δ (ppm): 144.3 (thiophene C3), 138.0 (thiophene C4), 111.8 (thiophene C2), 71.2 (thiophene C5), 34.2 (CH$_2$-Br), 32.9 (dodecyl C11), 29.74, 29.68, 29.62, 29.61, 29.55, 29.46, 29.3, 29.2 (dodecyl C7), 28.9 (dodecyl C9), 28.3 (dodecyl C10). HRMS (ESI+): *m/z*: 533.9093 (M$^+$); calcd for $C_{16}H_{25}Br_2IS$: 533.9007.

2.3. Synthesis of the Polymers

The synthesis of copolymer PHT*co*AHT was described previously [15].

Poly(3-dodecylthiophene-*co*-3-(12-bromododecyl)thiophene)(A). In a 200 mL reactor, *i*-PrMgCl (2 M in THF) was added slowly to THF (120 mL) at 0 °C. The absorption of the solution was followed in situ by an UV-Vis probe. The addition was continued until the absorption of organomagnesium between 250 and 270 nm was persistent. **1** (397 mg, 86.9 μmol) and **2** (84 mg, 15.6 μmol) were added. *i*-PrMgCl (2 M in THF) was added slowly to metallate not more than 90% of the monomer. Small volumes were taken from the medium and hydrolyzed with CD$_3$OD. The NMR spectra of these samples allowed to measure the rate of metallated monomers (singlet at 6.90 ppm, Figure 1). The mixture was heated to 20 °C and Ni(dppp)Cl$_2$ (3.78 mg, 7.16 μmol, 0.007 equiv.) was added. The polymerization was followed by the increase of the absorption at 440 nm. After it reached a plateau, the reaction was stopped with 100 μL of aqueous HCl (2 M). The solution volume was reduced of 80% by evaporation and the polymer was precipitated in methanol (10 × the volume of the remaining solution). The precipitate was centrifuged (9500 rpm, 2 h) and dried under vacuum for 24 h to yield copolymer **A** (234 mg, 83%). It was further purified by preparative GPC in CHCl$_3$. ^{1}H NMR (400 MHz, CDCl3): δ (ppm) 6.99 (s, 1H, thiophene C4–H), 3.39 (t, 0.33 H, *J* = 6.8 Hz, CH$_2$Br), 2.75–2.90 (m, 2H, thiophene-CH$_2$), 1.84 (p, 0.33 H, *J* = 6.9 Hz, **CH$_2$**CH$_2$Br), 1.66–1.78 (m, dodecyl C2–H$_2$), 1.50–1.17 (m, 18H, CH$_2$), 0.88 (m, 3H, CH$_3$). ^{13}C NMR (100 MHz, CDCl$_3$) δ (ppm): 140.0 (thiophene C3), 133.9 (thiophene C4), 130.6 (thiophene C2), 128.8 (thiophene C5), 34.1 (CH$_2$Br), 33.0 (bromododecyl C11), 32.1 (dodecyl C3), 30.7 (dodecyl C2), 29.9, 29.83, 29.76, 29.68; 29.54 (bromododecyl C9), 28.4 (bromododecyl C10), 22.8 (**C**H$_2$CH$_3$), 14.3 (CH$_3$). FTIR (ATR diamond) ν (cm^{-1}): 3400 (aromatic ν CH), 2956 ($ν_{as}$ CH$_3$), 2918 ($ν_{as}$CH$_2$), 2850 ($ν_s$CH$_2$), 1509 (aromatic νCC), 1466, 1455, 1377 (δCH$_3$), 1260, 1086, 1031; 818, 802, 719.
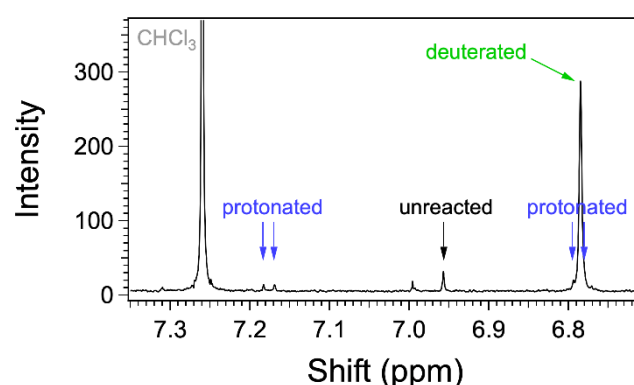

Figure 1. Measurement of the active monomer: an aliquot of the reaction medium was neutralized by CD$_3$OD. The active species is deuterated in position 5 and yields a singlet. The species yielding two doublets at 7.17 and 6.79 ppm comes from the deactivation of the magnesium by protonated impurities in the medium.

Poly(3-dodecylthiophene-*co*-3-(12-(4-(diphenylimino)phenoxy)dodecyl)thiophene) (B): K$_2$CO$_3$ (80.1 mg, 580 μmol, 10 equiv.), and 4-[(diphenylmethylene) amino]phenol

(78.5 mg, 283 µmol, 4.9 equiv.), Bu$_4$NBr (23.3 mg, 72.3 µmol, 1.25 equiv.), DMF (2 mL) and a solution of copolymer **A** (94.4 mg, ~58 µmol of bromododecyl) in THF (30 mL) were mixed in a pressure tube. The sealed tube was heated 96 h at 95 °C. THF was evaporated under vacuum and the crude was precipitated in MeOH (10 x its volume). The precipitate was centrifuged (9500 rpm) and dried for 24 h to afford polymer **B** (211 mg, 89% yield). ^{1}H NMR (400 MHz, CDCl$_3$): δ (ppm) 7.72 (d, 0.28 H, *J* = 7.2 Hz, imine phenyl), 7.47–7.33 (m, 0.42 H, imine phenyl), 7.25 (m, overlap with CHCl$_3$,imine phenyl), 7.11 (m, 0.28 H, imine phenyl), 6.98 (s, 1H, thiophene C4–H), 6.66 (m, 0.56 H, *J* = 8.4 Hz, aminophenol H), 3.83 (t, 0.28 H, *J* = 6.3 Hz, CH$_2$O), 2.81 (m, 2H, dodecyl C1-H$_2$), 1.51–1.87 (m, 2H, dodecyl C2-H$_2$), 1.10–1.51 (m, 18 H, dodecyl C3 to C11-H$_2$), 0.78–0.95 (m, 3H, CH$_3$). ^{13}C NMR (100 MHz, CDCl$_3$) δ (ppm): 167.8 (C=N), 155.5 (aryl C–O), 144.3 (aryl C–N), 140.2 (Ph$_2$CN phenyl C1), 140.0 (thiophene C3), 136.8 (Ph$_2$CN phenyl C4), 136.8, 133.7 (thiophene C5 HTHT). 130.6 (thiophene C2), 129.7, 129.3, 128.8 (thiophene C4), 128.6, 128.7, 133.7 (C2 thiophene), 128.3, 128.2, 125.7, 122.7, 114.5, 68.2 (CH$_2$O), 32.1 (**C**H$_2$CH$_2$CH$_3$). 30.7 (dodecyl C2), 29.89, 29.04, 29.75, 29.68, 29.61 29.55, 26.2 (**C**H$_2$CH$_2$CH$_2$-O), 22.8 (**C**H$_2$CH$_3$), 14.3 (CH$_3$). FTIR (ATR diamond) ν (cm^{-1}): 3054 (aromatic ν CH), 2953 (ν$_{as}$CH$_3$), 2917 (ν$_{as}$CH$_2$), 2848 (ν$_s$CH$_2$), 1607 (imine νCN), 1567, 1501, 1446, 1376 (δCH$_3$), 1315 (aryl C–N stretching), 1238 (ν C–O ether), 1167 (νC–O ether), 1028, 958, 828, 819 (aromatic oop δCH), 783, 720 (rCH$_2$), 693.

Poly(3-dodecylthiophene-*co*-3-(12-(4-aminophenoxy)dodecyl)thiophene) (PDT-co-ADT): copolymer **B** (50.8 mg, 28 µmol of imine) and hydroxylamine (50 wt.% in water, 71 mg, 1.07 mmol, 38 equiv.) were dissolved in THF (2 mL) and the mixture was stirred for 20 h at 50 °C. The polymer was precipitated in methanol, centrifuged (9500 rpm, 2 h) and dried for 24 h. A shiny violet solid was obtained (36.6 mg, 72% yield). ^{1}H NMR (400 MHz, CDCl$_3$) δ (ppm) 6.98 (s, 1H, thiophene CH, HTHT), 6.72 (d, 0.28H, *J* = 8.7 Hz, phenyl C2–H and C6–H), 6.62 (d, 0.28H, *J* = 8.7 Hz, phenyl C3–H and C5–H), 5.02 (s, NH$_2$), 3.85 (t, 0.28 H, *J* = 6.4 Hz, CH$_2$O), 2.81 (m, 2H, CH$_2$-thiophene HTHT), 1.71 (m, 2H, **C**H$_2$CH$_2$-thiophene), 1.48–1.18 (m, 18H, CH$_2$), 0.88 (t, *J* = 6.5 Hz, 3H, CH$_3$). ^{13}C NMR (400 MHz, CDCl$_3$) δ (ppm): 140.0 (C3 thiophene HT-HT), 133.8 (C5 thiophene HTHT). 130.5 (C2 thiophene HT-HT), 128.8 (C4 thiophene HT-HT). 116.5 (aniline C2, C6), 115.7 (aniline C3, C5), 32.0 (CH$_3$), 68.8 (CH$_2$O), 30.7 (**C**H$_2$CH$_2$-thiophene dodecyl), 30.7, 29.9, 29.8, 29.7, 29.6, 29.5, 22.9, 29.4 (**C**H$_2$CH$_2$CH$_3$), 26.3 (**C**H$_2$CH$_2$O), 22.9 (**C**H$_2$CH$_3$), 14.3 (CH$_3$). FTIR (ATR diamond) ν (cm^{-1}): 3359 (large, NH stretching), 3055 (aromatic νCH), 2949 (ν$_{as}$CH$_3$), 2918 (ν$_{as}$CH$_2$), 2849 (ν$_s$CH$_2$), 1625 (NH bend), 1562 (NH bend), 1510 and 1465 (aromatic νCC), 1377 (δCH$_3$), 1236 (νCO ether), 819 (oop aromatic CH), 719 (rCH$_3$).

2.4. Formation of the Polymer/SWNT Hybrids

HiPCO SWNTs (mean diameter 1.0 ± 0.2 nm) were purchased from NanoIntegris (Boisbriand, QC, Canada). They were dried at 250 °C under vacuum prior to use.

SWNT mother suspension: HiPCO SWNTs were dried at 250 °C under vacuum. 1.6 mg of the dry SWNTs were suspended in 5 mL of THF through tip sonication (5 min, 80 W, final concentration 0.32 mg/mL).

Formation of the non-covalent hybrids: A mother solution of polymer was prepared by dissolving 3.1 mg of PDT*co*ADT in 5 mL of THF (final concentration 0.62 mg/mL). A typical suspension for study of non-covalent nanohybrids is prepared by diluting 100 µL of this suspension in 5 mL of THF (final concentration 12.4 µg/mL, dissolved mass 62 µg), which led to an absorbance of 0.19 (5 mm cell). Fractions of 100 µL of the SWNT mother suspension (corresponding to 32 µg per fraction) were added to the copolymer solution, which is then tip sonicated. This operation is repeated until aggregation of the carbon nanotubes happened immediately after sonication.

Formation of the covalent hybrids: covalent functionalization was performed on a non-covalent dispersion of SWNTs with PDT*co*ADT. 0.8 mg of SWNTs were dispersed by sonication (5 min, 80 W) in 5 mL of a solution of PDT*co*ADT in THF (0.3 mg/mL, total amount 1.45 mg, corresponding to a SWNTs/polymer mass ratio of 0.55). This suspension
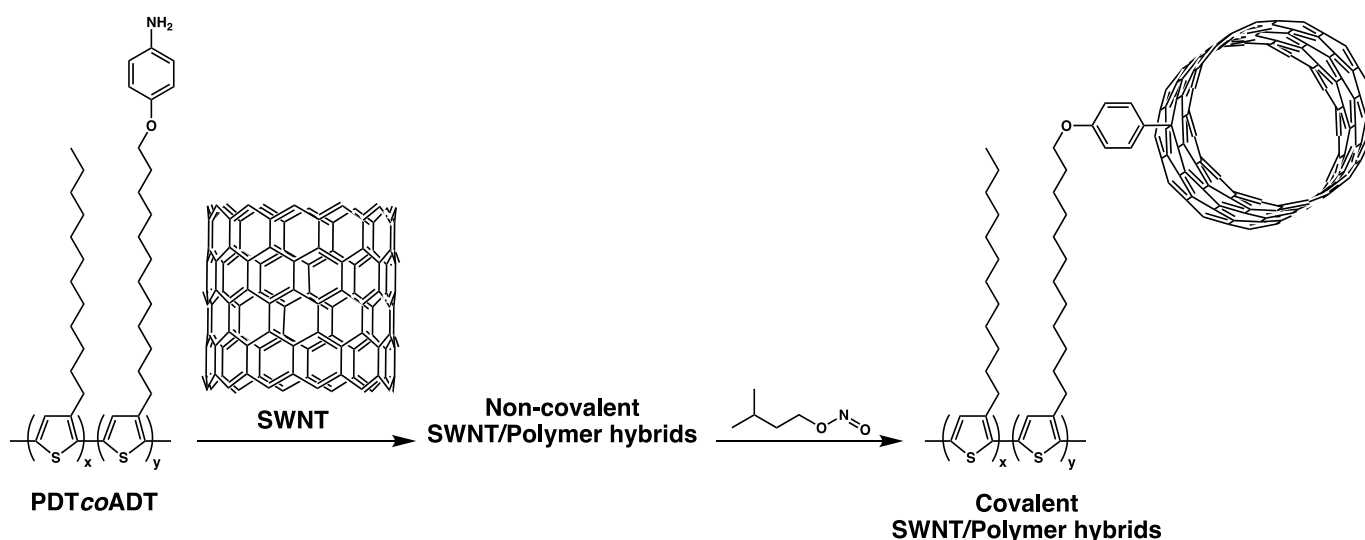
was degassed and put under nitrogen. 50 μL of isoamyl nitrite were added, the suspension was degassed anew and heated to 60 °C for 12 h. The supernatant of the final system was recovered and then analyzed.

Samples for Raman analysis: 50 μL of the recovered dispersions were deposited onto a glass plate by spin-coating. The obtained films were repeatedly washed with THF to eliminate the excess polymer.

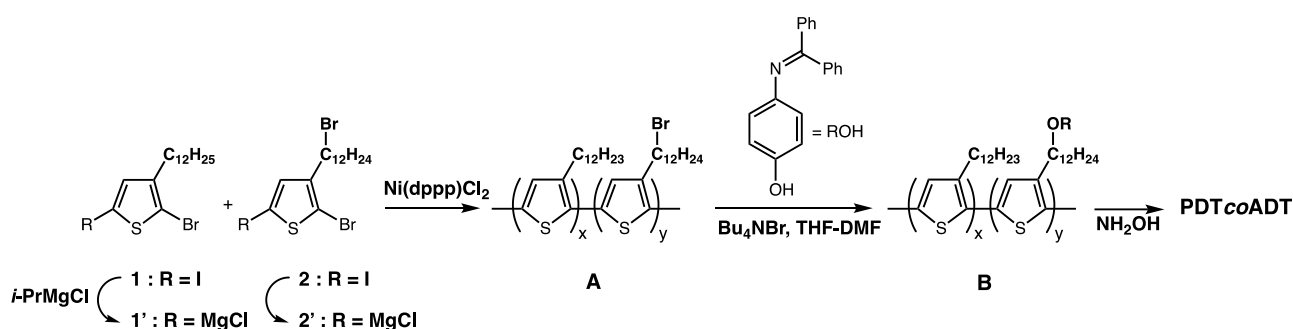## 3. Results and Discussion

3.1. Design of the Compounds

We aim at synthesizing a copolymer based on a poly(3-alkylthiophene) with side chains bearing aniline groups. As we have shown previously [15], when the alkyl chain is hexyl, this polymer is able to bind non-covalently with SWNTs, to form soluble polymer/SWNT hybrid complexes. The same hybrids heated in the presence of isoamyl nitrite react according to Tour's reaction: the aniline groups are transformed into a transitory diazonium that reacts with SWNTs to attach the phenyl of the aniline covalently to the SWNTs walls (Scheme 1). In the present work, we synthesize a new polymer with dodecyl side chains, i.e., twice longer than in hexyl analogues.

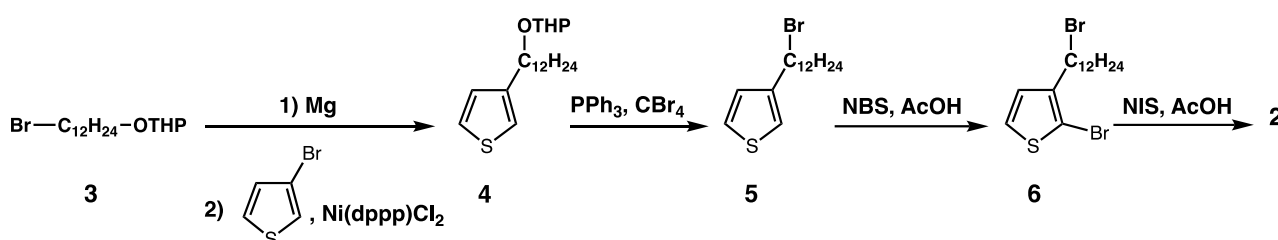**Scheme 1.** Structure of the targeted copolymers and their reaction with SWNTs.

3.2. Syntheses of the Monomers and Polymers

The copolymer was synthesized first by copolymerizing 2-bromo-3-dodecyle-5-iodothiophene **1** and its end brominated analogue **2** (Scheme 2) by the Grignard metathesis (GRIM) method [19,20].

Scheme 2. Synthesis of the PDT*co*ADT copolymer.

In a first step the monomers **1** and **2** were synthesized (Scheme 3) and then polymerized to afford polymer **A** bearing bromide at the end of the side chains (Scheme 2). As shown before [21], copolymerization with the bromo analogue is possible, and the end bromide does not interfer with the formation of the organomagnesium [21]. The choice of the iodine in position 5 adds a step to the synthesis of the monomer; but as shown by Catala et al. [22], it increases the regioselectivity of the metallation and subsequent polymerization. Moreover, both monomers have close reactivity, and we have shown that the composition of the polymer follows that of the feed mixture monomer [15], which suggests that the yielded polymer is a random copolymer. By the GRIM method, Yang et al. have also obtained random copolymers from thiophene based monomers with even larger structural differences than **1** and **2** [23].

Scheme 3. Synthesis of the monomer **2**.

The monomers were synthesized by coupling first the organomagnesium of Br-$C_{12}H_{24}$-OTHP with 3-bromothiophene, with Ni(dppp)Cl_2 as the catalyst (Scheme 3). The reaction proceeds with a fair yield (about 67%), but the compound **4** has a low polarity and has the same R_f as two byproducts (Br-$C_{12}H_{24}$-OTHP and $C_{12}H_{25}$-OTHP) in cyclohexane. Therefore compound **4** was not separated from these products but transformed in the next steps. The THP ether was converted into bromide, and the resulting compound **5** was brominated selectively in position 2 and iodinated in position 5. Compounds **5, 6,** and **2** are less polar than **4**, but can be purified by flash chromatography.

The monomer **1** and **2** were metallated with *i*-PrMgCl. The formation of the resulting organomagnesium was followed by taking aliquots from the reaction and quenching them with CD_3OD. The species **1′** and **2′** are deuterated in position 5 and the resulting compound, has only one proton yielding a singlet at 6.78 ppm, the major peak in this area (Figure 1). The unreacted compound **2** can be identified by a singlet at 6.96 ppm. Another present species is characterized by two doublets: the first at 7.18 ppm, and the second which overlaps with the main peak. It corresponds to the organomagnesium that was hydrolyzed by protonated impurities in the mixture before quenching. The resulting compound has two protons in position 4 and 5 and is clearly distinct from the one coming from the deactivation of the active species by CD_3OD. It allows to measure exactly the ratio of active species and adapt the amount of catalyst to control the length of the polymer.

The polymerization is initiated by the addition of the catalyst, and the propagation is followed in situ by UV by measuring the absorbance at 445 nm. The obtained polymer **A** has a M_n of 41,000 (DP$_n$ ~ 155) as determined by MALS, and a polymolecularity index of 1.42 (Figure 2a). The polymer was tentatively purified by recycling SEC in chloroform. The mass distribution was slightly improved with a polymolecularity of 1.37. The ratio of bromide in the polymer was measured by integrating of the triplet at 3.41 ppm characteristic of CH_2Br, and the massif centered at 2.45 ppm from the CH_2 in alpha of the thiophene (Figure 2b). From the ratio of both, one measures a rate of bromine in the polymer of $16.5 \pm 2\%$. This rate represents an average of 25 brominated side chains per polymer chain.

The functionalized side chains were etherified by an excess of 4-aminophenol, *N*-protected as its diphenylimine, with a phase transfer catalyst (Scheme 2). The rate of substitution in the final polymer is quantitative as shown by the total disappearance of the CH_2Br signals in NMR. The aniline was deprotected by transamination with hydroxylamine

in THF to afford the final polymer. It must be stored at 0 °C under Ar since it tends to degrade and crosslink.
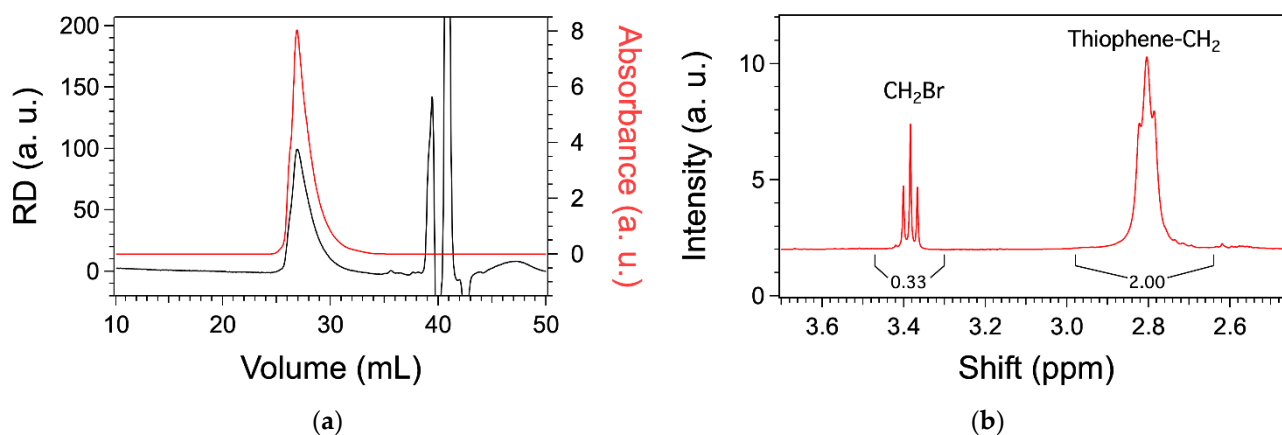

Figure 2. Characterization of copolymer A (41,000 g/mol) (**a**) SEC traces: RD and UV absorbance at 448 nm; (**b**) Enlarged NMR spectrum showing the proton in benzylic position and next to Br, with the corresponding integrals.

3.3. Formation and Study of the Non-Covalent Copolymer/SWNT Hybrids

The non-covalent functionalization of SWNTs was studied by adding repeatedly the same amount of SWNTs (32 µg) to a solution of PDT*co*ADT (62 µg in 5 mL, conc. 12.4 µg/mL). During the first additions, the resulting suspensions are stable for a few hours; after a given number of additions, corresponding to a threshold SWNT/PDT*co*ADT mass ratio, the SWNTs are no longer suspended and precipitate immediately.

After each addition of SWNTs to PDT*co*ADT, the suspensions were studied by UV-Vis-NIR (Figure 3). The starting polymer solution, without SWNTs shows only one broad peak at 450 nm. This peak represents the free copolymer in solution. When the amount of SWNTs increases, this peak decreases. At the same time, we observe an increase of the background absorption corresponding to the tail of the SWNTs π-plasmon absorption (around 180 nm), the appearance of two sets of peaks between 700 and 1500 nm, corresponding to SWNTs optical transitions, and the appearance of peaks between 500 and 650 nm. These latter peaks are characteristic of aggregates of regioregular P3HT formed by π-stacked planar and extended polymer chains [24]. The absence of these bands in the starting solution shows that PDT*co*ADT is fully soluble in THF at this concentration. The appearance of these bands in the presence of SWNTs strongly suggests π-π interactions between the copolymer chains and the SWNTs in the hybrids. In the spectra measured during these experiments, the characteristic features of both polymer aggregates and SWNTs do not change significantly, indicating a similar molecular array at the interface of the hybrids.

For the maximal SWNT/PDT*co*ADT mass ratio, the contribution of the peak of the free polymer at 450 nm is less than 10% of the intensity of the signal (Figure 4). It indicates that all the polymer chains are adsorbed on SWNTs. As found previously [15], for the analogue copolymer PHT*co*AHT, with hexyl side chains, with the same aniline ratio and a M_n of 36,000 (DP$_n$ of 200), the contribution of the free polymer at 450 nm is of about 30% of the intensity of the signal for a critical mass ratio of 1.26. In summary, the first effect of lengthening the side chain is a better stacking of the polymer chains on the SWNTs.

The threshold ratio above which spontaneous flocculation occurs is 2.9 ± 0.6 mg of SWNTs per mg of PDT*co*ADT. This ratio corresponds to 780 mg of SWNTs per mmol of PDT*co*ADT. As shown previously [15], for the hexyl analogue, the critical ratio is of 230 mg of SWNTs per mmol of PHT*co*AHT. It shows that the dodecyl analogue solubilizes 3.3 times more SWNTs than the hexyl analogue. This difference is attributed to the better solubility in THF of the dodecyl copolymer due to more flexibility of the polymer backbone and its side chains in solution, which facilitates the optimization of their configuration to wrap around the SWNTs [18].
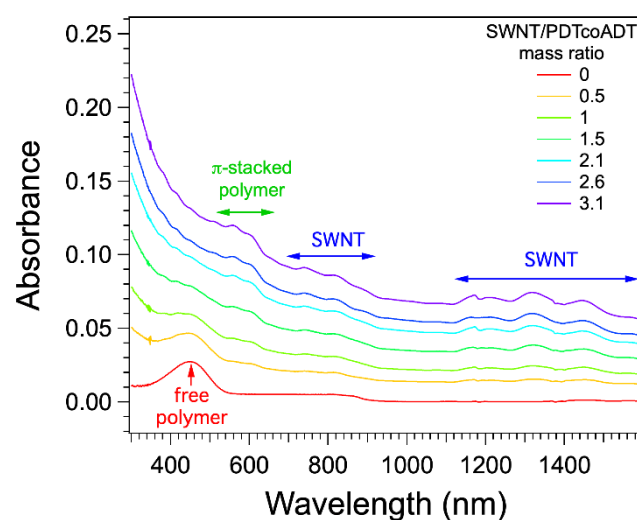
Figure 3. Evolution UV-Vis-NIR spectra of a solution of PDT*co*ADT (0.62 μg, conc. 0.124 μg/mL) after repeated additions of the same amount of SWNTs (0.32 μg).
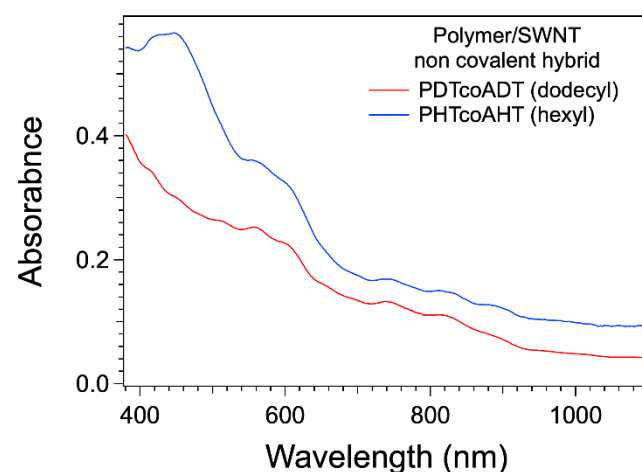

Figure 4. Spectra of the non-covalent nanohybrids before the onset of flocculation for PDT*co*ADT (red, SWNTs/polymer mass ratio = 3.1) and comparison with the spectrum of PHT*co*AHT (blue, SWNTs/polymer mass ratio = 1.26, from reference [15]).

In parallel to their absorbance, the photoluminescence of the non-covalent PDT*co*ADT hybrids was measured during their formation (Figure 5). When the mere copolymer, without SWNT, is excited at 450 nm, it gives rise to a fluorescence emission which peaks at 570 nm. Upon addition of incremental amounts of SWNTs, we observe a reduction of emission intensity concomitant to the reduction of the free polymer contribution in the absorption spectrum, but no change of the shape of the photoluminescence spectra. Moreover, one observes no characteristic emission of polymer aggregates at 630 and 690 nm [25], even upon excitation at 560 nm, corresponding to the maximum of their optical absorption. These results, similar to those obtained with PHT*co*AHT [15], confirm that the aggregates form on the SWNTs surface and have their fluorescence quenched by their interaction with these species.
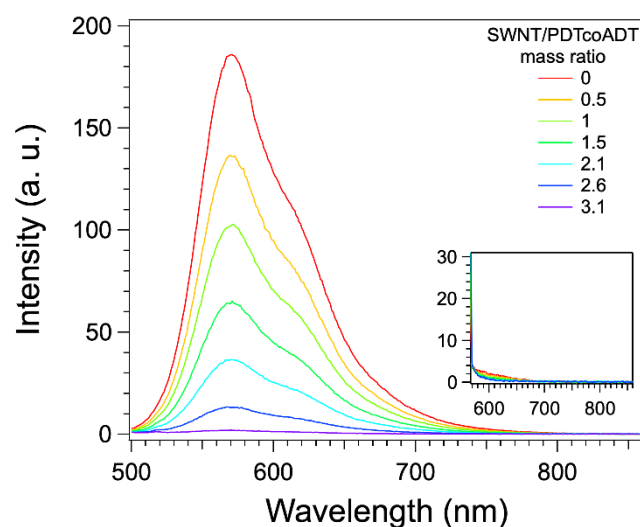
Figure 5. Photoluminescence spectra of the suspensions of non-covalent hybrids for different SWNTs/PDT*co*ADT mass ratios; excitation at 450 nm; inset: excitation at 560 nm, at the same scale, showing no PL.

3.4. Formation of the Covalent Hybrids

Covalent functionalization is performed starting from the non-covalent nanohybrids. In order to conduct the reaction on stable suspensions, the SWNTs/copolymer mass ratio is set at 0.55, well below the flocculation threshold of 2.9 found in the previous section. We use a higher concentration of both species for increasing the final amount of covalent nanohybrids.

After the reaction, the suspensions are stable for a few days. Therefore, lengthening the side chains lowers the stability of the covalent hybrids: the hybrids obtained with the hexyl analogue PHT*co*AHT were stable for a few weeks. This lower stability was unexpected. Moreover, with the dodecyl polymer most of the material precipitates under centrifugation, which prevents separating reacted from unreacted SWNTs. For this reason, the spectroscopic characterizations have been performed on the raw suspensions (without centrifugation).

After the reaction, the UV-Vis spectrum of the sample still exhibits the absorption signals of both copolymer and SWNTs but not the characteristic features of PDT*co*ADT aggregates between 500 and 650 nm. Thus, the reaction induces a change in the organization of the polymer in the covalent hybrids compared to the non-covalent ones (Figure 6).
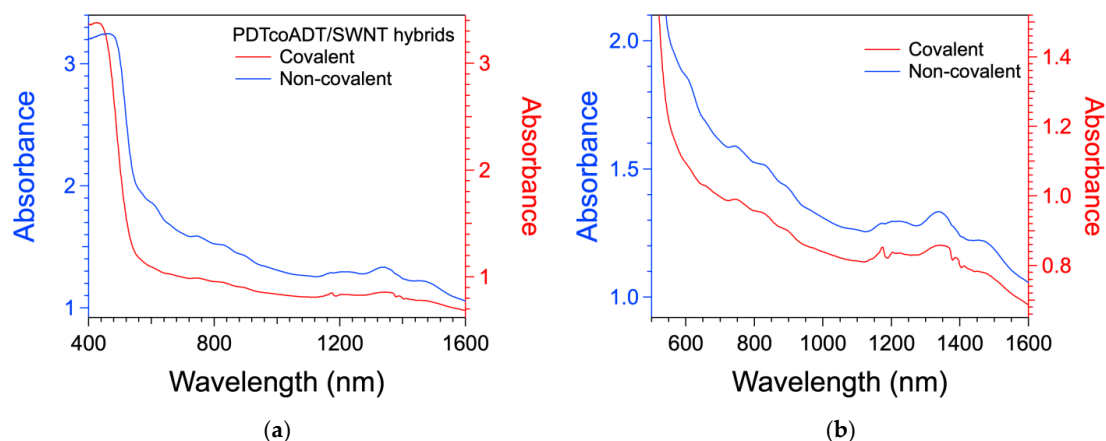

Figure 6. (**a**) UV-Vis spectra of the non-covalent (blue line, left scale) and covalent (red line, right scale) PDT*co*ADT/SWNT nanohybrids. Since higher concentrations were used, the absorption by the free polymer and the isoamyl nitrite saturates the signal at low wavelengths. (**b**) Same spectra focused on the polymer aggregates and SWNTs absorption.

The results of Raman spectroscopy allow the study of the conformation of the polymer onto the surface of SWNTs; they are shown in Figure 7. The modes of SWNTs are the D band around 1320 cm^{-1} and the G modes in the 1500–1600 cm^{-1} range. For the three samples they have close frequencies and the D/G intensity ratios are the same. This is in agreement with the expected low amount of grafting bonds (10^{-3} per C atom) and a large distance between defects, of the order of 2–3 nm [7,26]. On the contrary, the lineshape of the modes of the PDT*co*ADT, located in the 1350–1500 cm^{-1} range, and assigned to the C–C and C=C stretching modes, are different in the non-covalent and covalent samples (Figure 8b). This indicates clearly that the organization of the copolymer is not the same in both hybrids [27].
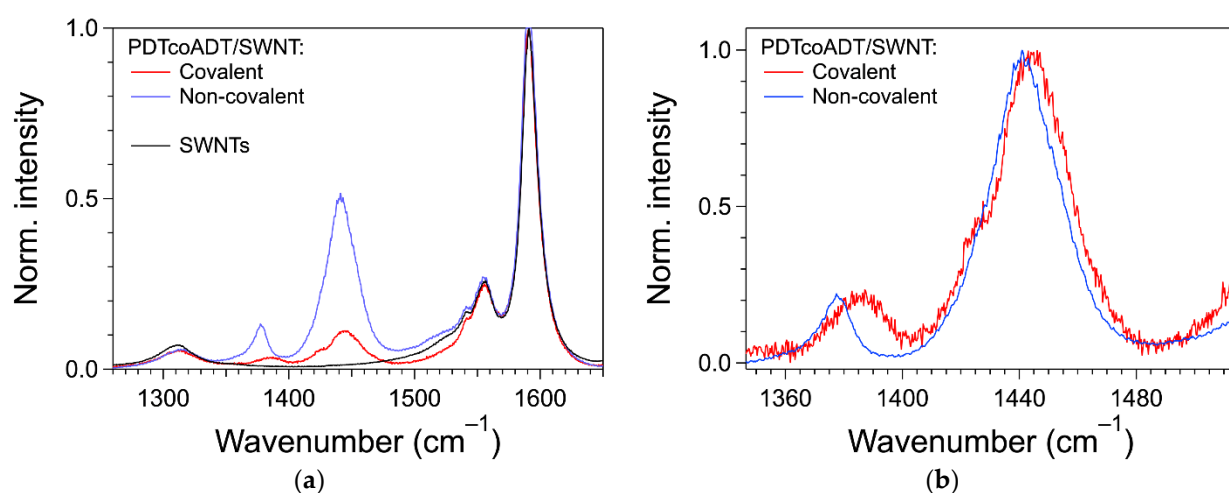

Figure 7. (**a**) High frequency Raman spectra (excitation at 633 nm) of pristine SWNTs (black) and of covalent (red) and non-covalent (blue) PDT*co*ADT/SWNT nanohybrids. The spectra are normalized by the intensity of the G mode at 1590 cm^{-1}. (**b**) same spectra focused on the C-C and C=C vibration modes, normalized by their intensity at 1445 cm^{-1}.

Figure 8. (**a**) High frequency Raman spectra (excitation at 633 nm) of covalent PDT*co*ADT/SWNTs (red) and covalent PHT*co*AHT/SWNTs (blue) nanohybrids. The spectra were normalized by the intensity of the G mode at 1590 cm^{-1}. (**b**) same spectra focused on the C-C and C=C vibration modes, normalized by their intensity at 1445 cm^{-1}.
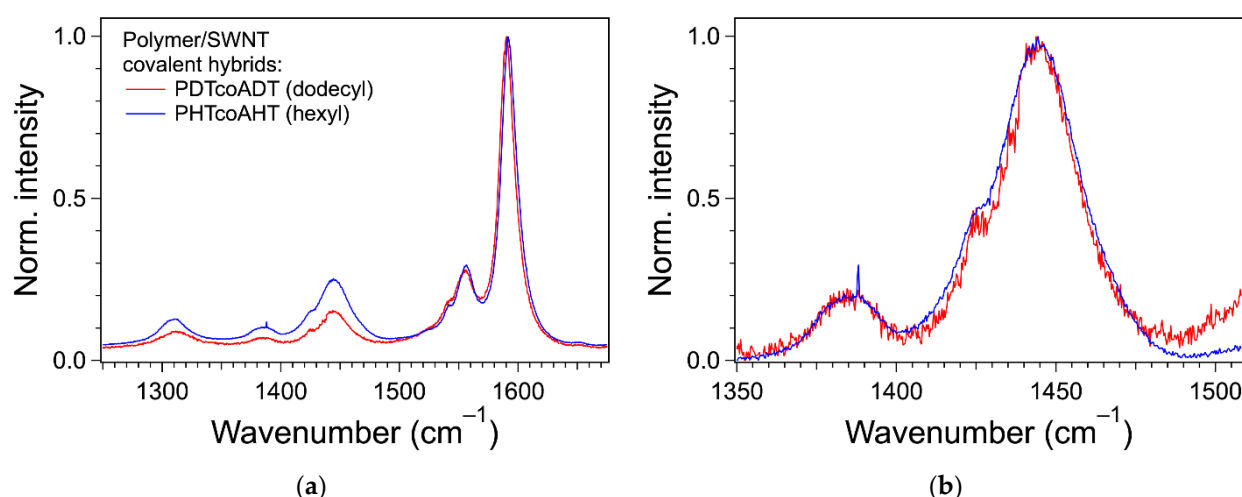
The intensity of the PDT*co*ADT signal is higher for the non-covalent nanohybrid than for the covalent one. This is in agreement with the formation of polymer aggregates in the non-covalent nanohybrids and their absence in the covalent nanohybrids, as observed by UV-Vis. The shift and broadening of the mode at 1380 cm^{-1}, the small upshift of the mode at 1450 cm^{-1}, and the appearance of a shoulder on its left side have been interpreted

by a loss of the molecular order of PHT*co*AHT chains in the covalent nanohybrids [15]. This result is due to the absence of π-stacking of the thiophene units onto the SWNTs because, after covalent grafting, the appended aniline acts as a spacer between SWNTs and the PHT*co*AHT backbone. Since the spectra of the covalent PDT*co*ADT/SWNTs are close to those of hexyl analogues, we conclude that the polymer backbones adopt a similar conformation in both systems (Figure 8).

Therefore, the lower solubility of covalent PDT*co*ADT/SWNTs compared to that of PHT*co*AHT/SWNTs cannot be attributed to a difference in the polymer conformation. It could be attributed to a better exfoliation of SWNTs by PHT*co*AHT than by PDT*co*ADT, PDT*co*ADT may be able to solubilize larger but non-exfoliated bundles by non-covalent functionalization. This would agree with PDT*co*ADT solubilizing 3 times more SWNTs than the hexyl analogues. However, this contradicts the findings of Lee et al. [18]. Another explanation for the lower solubility of the covalent PDT*co*ADT/SWNTs is that longer alkyl chains could favor bridging reaction of neighbouring tubes during the covalent derivatization. This reactivity may be underpinned also by a higher solubility of the polymers in the solvent, and weaker interaction between the polymer and the tubes in the non-covalent hybrids.

4. Conclusions

The copolymer PDT*co*ADT was synthesized at the scale of hundreds of mg by copolymerization of 3-dodecylthiophene and its aniline appended analogue. It was obtained with high regioregularity. This polymer is able to form both non-covalent and covalent hybrids. In the non-covalent nanohybrids, the polymer forms π-stacked aggregates at the surface of the nanotubes, while it is no longer π-stacked in the covalent hybrids. This behavior is the same as for the analogue polymer with shorter hexyl side chains, PHT*co*AHT, previously reported. The new results are that lengthening the side chains resulted in the dispersion of a higher amount of SWNTs. Lengthening the side-chain also increases the proportion of polymer chains π-stacked at the surface of the tube. Very surprisingly the PDT*co*ADT/SWNTs covalent nanohybrids were insoluble in THF, contrary to PHT*co*AHT/SWNTs. From our spectroscopic studies, this result cannot be explained by the conformation of the polymer at the surface of nanotubes, and further studies will be conducted to address this difference of behavior.

Author Contributions: Conceptualization, P.P. and P.J.M.; methodology, P.P. and P.J.M.; investigation, F.W.K. and J.-P.L.; writing—original draft preparation, F.W.K. and P.J.M.; writing—review and editing, F.W.K., J.-P.L., M.P., P.P., and P.J.M.; supervision, M.P., P.P., and P.J.M.; funding acquisition, M.P. and P.P. All authors have read and agreed to the published version of the manuscript.

Institutional Review Board Statement: Not applicable.

Informed Consent Statement: Not applicable.

Data Availability Statement: The data presented in this study are available on request from the corresponding author. The data are not publicly available due to lack of dedicated server.

Conflicts of Interest: The authors declare no conflict of interest.

References

1. Campidelli, S. Click Chemistry for Carbon Nanotubes Functionalization. *Curr. Org. Chem.* **2011**, *15*, 1151–1159. [CrossRef]
2. Li, H.; Cheng, F.; Duft, A.M.; Adronov, A. Functionalization of Single-Walled Carbon Nanotubes with Well-Defined Polystyrene by "Click" Coupling. *J. Am. Chem. Soc.* **2005**, *127*, 14518–14524. [CrossRef] [PubMed]

3.   Ma, P.-C.; Siddiqui, N.A.; Marom, G.; Kim, J.-K. Dispersion and functionalization of carbon nanotubes for polymer-based nanocomposites: A review. *Compos. Part A Appl. Sci. Manuf.* **2010**, *41*, 1345–1367. [CrossRef]

4.   Nurazzi, N.M.; Sabaruddin, F.A.; Harussani, M.M.; Kamarudin, S.H.; Rayung, M.; Asyraf, M.R.M.; Aisyah, H.A.; Norrrahim, M.N.F.; Ilyas, R.A.; Abdullah, N.; et al. Mechanical Performance and Applications of CNTs Reinforced Polymer Composites—A Review. *Nanomaterials* **2021**, *11*, 2186. [CrossRef]

5.   Nurazzi, N.M.; Asyraf, M.R.M.; Khalina, A.; Abdullah, N.; Sabaruddin, F.A.; Kamarudin, S.H.; Ahmad, S.; Mahat, A.M.; Lee, C.L.; Aisyah, H.A.; et al. Fabrication, Functionalization, and Application of Carbon Nanotube-Reinforced Polymer Composite: An Overview. *Polymers* **2021**, *13*, 1047. [CrossRef] [PubMed]

6.   Chen, Y.; Marty, L.; Bendiab, N. New Light on Molecule–Nanotube Hybrids. *Adv. Mater.* **2019**, *31*, 1902917. [CrossRef] [PubMed]

7.   Piao, Y.; Meany, B.; Powell, L.R.; Valley, N.; Kwon, H.; Schatz, G.C.; Wang, Y. Brightening of carbon nanotube photoluminescence through the incorporation of sp3 defects. *Nat. Chem.* **2013**, *5*, 840–845. [CrossRef] [PubMed]

8.   Bahr, J.L.; Tour, J.M. Highly Functionalized Carbon Nanotubes Using in Situ Generated Diazonium Compounds. *Chem. Mater.* **2001**, *13*, 3823–3824. [CrossRef]

9.   Strano, M.S.; Dyke, C.A.; Usrey, M.L.; Barone, P.W.; Allen, M.J.; Shan, H.; Kittrell, C.; Hauge, R.H.; Tour, J.M.; Smalley, R.E. Electronic Structure Control of Single-Walled Carbon Nanotube Functionalization. *Science* **2003**, *301*, 1519–1522. [CrossRef]

10.   Dyke, C.A.; Tour, J.M. Covalent functionalization of single-walled carbon nanotubes for materials applications. *J. Phys. Chem. A* **2004**, *108*, 11151–11159. [CrossRef]

11.   Berger, F.J.; Lüttgens, J.; Nowack, T.; Kutsch, T.; Lindenthal, S.; Kistner, L.; Müller, C.C.; Bongartz, L.M.; Lumsargis, V.A.; Zakharko, Y.; et al. Brightening of Long, Polymer-Wrapped Carbon Nanotubes by sp 3 Functionalization in Organic Solvents. *ACS Nano* **2019**, *13*, 9259–9269. [CrossRef] [PubMed]

12.   Liu, J.; Ye, Y.; Xue, Y.; Xie, X.; Mai, Y.-W. Recent advances in covalent functionalization of carbon nanomaterials with polymers: Strategies and perspectives. *J. Polym. Sci. Part A Polym. Chem.* **2017**, *55*, 622–631. [CrossRef]

13.   Abousalman-Rezvani, Z.; Eskandari, P.; Roghani-Mamaqani, H.; Salami-Kalajahi, M. Functionalization of carbon nanotubes by combination of controlled radical polymerization and "grafting to" method. *Adv. Colloid Interface Sci.* **2020**, *278*, 102126. [CrossRef] [PubMed]

14.   Díez-Pascual, A.M. Chemical Functionalization of Carbon Nanotubes with Polymers: A Brief Overview. *Macromol* **2021**, *1*, 64–83. [CrossRef]

15.   Wasem Klein, F.; Lamps, J.-P.; Raoui, M.; Paillet, M.; Sauvajol, J.-L.; Mésini, P.J.; Petit, P. Design and synthesis of aniline-appended P3HT for single step covalent functionalisation of carbon nanotubes. *Polym. Chem.* **2020**, *11*, 6319–6327. [CrossRef]

16.   Gomulya, W.; Costanzo, G.D.; De Carvalho, E.J.F.; Bisri, S.Z.; Derenskyi, V.; Fritsch, M.; Fröhlich, N.; Allard, S.; Gordiichuk, P.; Herrmann, A.; et al. Semiconducting single-walled carbon nanotubes on demand by polymer wrapping. *Adv. Mater.* **2013**, *25*, 2948–2956. [CrossRef] [PubMed]

17.   Fong, D.; Adronov, A. Recent developments in the selective dispersion of single-walled carbon nanotubes using conjugated polymers. *Chem. Sci.* **2017**, *8*, 7292–7305. [CrossRef]

18.   Lee, H.W.; Yoon, Y.; Park, S.; Oh, J.H.; Hong, S.; Liyanage, L.S.; Wang, H.; Morishita, S.; Patil, N.; Park, Y.J.; et al. Selective dispersion of high purity semiconducting single-walled carbon nanotubes with regioregular poly(3-alkylthiophene)s. *Nat. Commun.* **2011**, *2*, 541–548. [CrossRef]

19.   Miyakoshi, R.; Yokoyama, A.; Yokozawa, T. Catalyst-Transfer Polycondensation. Mechanism of Ni-Catalyzed Chain-Growth Polymerization Leading to Well-Defined Poly(3-hexylthiophene). *J. Am. Chem. Soc.* **2005**, *127*, 17542–17547. [CrossRef]

20.   Iovu, M.C.; Sheina, E.E.; Gil, R.R.; McCullough, R.D. Experimental Evidence for the Quasi-"Living" Nature of the Grignard Metathesis Method for the Synthesis of Regioregular Poly(3-alkylthiophenes). *Macromolecules* **2005**, *38*, 8649–8656. [CrossRef]

21.   Tahar-Djebbar, I.; Nekelson, F.; Heinrich, B.; Donnio, B.; Guillon, D.; Kreher, D.; Mathevet, F.; Attias, A.-J. Lamello-Columnar Mesophase Formation in a Side-Chain Liquid Crystal π-Conjugated Polymer Architecture. *Chem. Mater.* **2011**, *23*, 4653–4656. [CrossRef]

22.   Vallat, P.; Lamps, J.P.; Schosseler, F.; Rawiso, M.; Catala, J.M. Quasi-Controlled Polymerization through a Nickel Catalyst Process of a Functionalized Thiophene Monomer: Kinetic Studies and Application to the Synthesis of Regioregular Poly(thiophene-3-acetic acid). *Macromolecules* **2007**, *40*, 2600–2602. [CrossRef]

23.   Yang, Y.-L.; Lee, Y.-H.; Lee, Y.-P.; Chiang, C.-J.; Shen, C.; Wu, C.-C.; Ohta, Y.; Yokozawa, T.; Dai, C.-A. Synthesis and characterization of poly(3-hexylthiophene)–poly(3-hexyloxythiophene) random copolymers with tunable band gap via Grignard metathesis polymerization. *Polym. Int.* **2014**, *63*, 2068–2075. [CrossRef]

24.   Spano, F.C.; Silva, C. H- and J-Aggregate Behavior in Polymeric Semiconductors. *Annu. Rev. Phys. Chem.* **2014**, *65*, 477–500. [CrossRef] [PubMed]

25.   Rumbles, G.; Samuel, I.D.W.; Magnani, L.; Murray, K.A.; DeMello, A.J.; Crystall, B.; Moratti, S.C.; Stone, B.M.; Holmes, A.B.; Friend, R.H. Chromism and luminescence in regioregular poly(3-dodecylthiophene). *Synth. Met.* **1996**, *76*, 47–51. [CrossRef]

26.   Giulianini, M.; Waclawik, E.R.; Bell, J.M.; Crescenzi, M.D.; Castrucci, P.; Scarselli, M.; Diociauti, M.; Casciardi, S.; Motta, N. Evidence of Multiwall Carbon Nanotube Deformation Caused by Poly(3-hexylthiophene) Adhesion. *J. Phys. Chem. C* **2011**, *115*, 6324–6330. [CrossRef]

27.   Wood, S.; Hollis, J.R.; Kim, J.-S. Raman spectroscopy as an advanced structural nanoprobe for conjugated molecular semiconductors. *J. Phys. D Appl. Phys.* **2017**, *50*, 073001. [CrossRef]